INDIAN JOURNAL OF SCIENCE AND TECHNOLOGY

RESEARCH ARTICLE

Photoluminescence Interaction of Alkali Fluoride Over Alkali Oxide in Nd^{3+} Doped Glasses for NIR Applications

Basavaraj Gurav[1], G B Devidas[1]*, Ashok Dinkar[1], Shrikant Biradar[1], R Rajaramakrishna[2,3]

1 Department of Physics, Jnana Sahyadri, Kuvempu University, Shankarghatta, Shimoga, 577451, Karnataka, India
2 Center of Excellence in Glass Technology and Materials Science (CEGM), Nakhon Pathom Rajabhat University, 73000, Nakhon Pathom, Thailand
3 Department of Post Graduate Studies and Research in Physics, The National College, Jayanagar, Bengaluru, 560070, Karnataka, India

OPEN ACCESS

Received: 08-12-2022
Accepted: 22-12-2022
Published: 24-01-2023

Citation: Gurav B, Devidas GB, Dinkar A, Biradar S, Rajaramakrishna R (2023) Photoluminescence Interaction of Alkali Fluoride Over Alkali Oxide in Nd^{3+} Doped Glasses for NIR Applications . Indian Journal of Science and Technology 16(3): 230-238. https://doi.org/10.17485/IJST/v16i3.2367

* **Corresponding author**.

devidasgb02@gmail.com

Funding: None

Competing Interests: None

Published By Indian Society for Education and Environment (iSee)

ISSN
Print: 0974-6846
Electronic: 0974-5645

Abstract

Background/Objectives: $23CaO + 10Al_2O_3 + (51 - x)B_2O_3 + 6BaF_2 + 10Na_2O + xNd_2O_3$ glasses were designed for understanding the optical properties of the emission, such as absorption, lifetime, and quantum efficiencies (QEs) of the glasses. **Methods:** The glasses were synthesized using the conventional melt-quenching technique at 1150^0C. The amorphous nature of the samples was confirmed by x-ray diffraction studies. **Findings:** The radiative QE (η) obtained from the radiative lifetime by Judd-Ofelt analysis, as well as directly measured lifetime using a 582 nm were measured and compared with other reported literature. **Novelty:** The present work focuses on the replacement of fluorine ions to their alkali content and studied their stimulated emission cross section. The stimulated emission cross-section shows σ_{emi}=25.3x10^{-21}cm^2 and σ_{emi}=18.5x10^{-21}cm^2 for oxide (R1) and oxy-fluoride glasses (F2) with 0.5mol% Nd_20_3 content respectively. The stimulated emission cross section σ_{emi}=29.9x10^{-21}cm^2 and σ_{emi}=32.5x10^{-21}cm^2 for oxide (F1) and oxy-fluoride (A3) glasses with 1.0mol% Nd_20_3 content respectively. The data clearly suggests that addition of higher fluorine content in the glasses are suitable for NIR solid state device applications.

Keywords: Nd 3+ ions; JOtheory; Radiative properties; photoluminescence; Borate glass

1 Introduction

The use of Nd^{3+} glasses in the realm of technology has increased especially for applications involving photonic and solid-state devices. For lasers, amplifiers, etc., rare-earth ions-doped glass is more appropriate. Among all the rare-earth ions, Nd^{3+} finds in the field of infrared

optical communication and laser due to their efficient infrared $^4\mathbf{I}_{9/2,11/2,13/2}$ with the emission at wavelengths around 946, 1064 and 1315 nm. The oxyfluoride glasses are found to have advantages of both oxide and fluoride glasses [1,2].

In general, oxide glasses have good chemical resistance and stability, while fluoride glasses have very low phonon energies. However, when fluoride is replaced with oxygen, the structure and connectivity of the glass are affected, and as a result, they are better suited to working in the ultraviolet spectrum and as laser materials [3].

Among all glasses, borate glasses are being studied because of their very intriguing properties that change with variations in the cation modifier content and its size with these variations being well related to glass structure modification. These glasses also have good solubility and high transparency, act as a dopant host and are responsible for the intrinsic emission, and can be used in a variety of applications, including lasers and solid-state lighting, etc [4,5].

M. Djmal et.at (2020), have investigated Nd3+ ion doped Zn-Al-Ba borate oxide glasses and reported that their glasses are applicable for NIR emitting devices [6]. In present work instead of oxide, the addition of fluoride which enhances luminescence properties.

Mauricio Rodriguez Chilanza, et. al (2021), had investigated oxy-fluoroborate glasses doped with Nd^{3+} and their results shows their glasses are applicable for thermoluminescence [4].

P. Rekha rani,et.al (2020), had investigated B_2O_3-BaF_2-PbF_2-Al_2O_3 glasses. They have shown quantum efficiency is 16% for BaPbAlFBNd2.5 glass [7]. In our cases we investigated quantum efficiency observed 22 to 47%. its more supportive to NIR- solid state device applications at 1.06μm.

2 Methodology

The glass sample with composition of $23CaO; 10Al_2O_3; (51-X)B_2O_3; 6BaF2; 10Na_2O; XNd_2O_3$

Where X=0.5, and 1.0, (coded as CaAlBBaFNaNd0.5), (coded as CaAlBBaFNaNd1.0), $23CaO; 10Al_2O_3$; (51-X) B_2O_3; 6BaF; 10NaF; XNd_2O_3 where X=0.5, (coded as CaAlBBaFNaFNd0.5), $23CaO; 10Al_2O_3$; (51-X) B_2O_3; 6BaO; 10NaF; XNd_2O_3 where X=1.0(coded as CaAlBBaNaFNd1.0) mol% concentrations prepared by conventional melt quenching technique. The oxide chemicals with the high purity of $CaCO_3$, Al_2O_3, H_3BO_3, $BaCO_3$, Na_2CO_3, BaF_2, NaF and Nd_2O_3 were well mixed on pestle mortar and grind to fine powder till, it obtained a homogeneous mixture and weighed to 15 grams, a porcelain crucible with well grinded oxides was used to place the uniform mixture in electrical muffle furnace. Density (ρ) measurements on glass samples were performed using the Archimedes technique using toluene as the immersion solvent. The prepared mixture was then heated at 1150^0 C for 3hours, the homogeneous oxides melt remained and then swifty dispensed into stainless steel block that had been pre - heated, and it was quenched to create uniform thick glass samples. To reduce thermal stress, the glass underwent an entire day of annealing at 550^0C before being allowed to cool gradually to ambient temperature. The powdered approach was utilized to capture the X-ray diffraction pattern of glass samples. Cu_k, with a wavelength of 1.54 nm, was employed as a source in the Diffractometer. The acquired glass sample were shaped for characterization. by being cut and polished. Using Perkin Elmer lambda 950 UV/VIS/NIR spectrophotometer, the optical absorption spectra of present glass were measured in UV/VIS/NIR region of 250-2500nm. The photoluminescence spectra were recorded using near-infrared spectrophotometers (Quanta Master (QM)-300, PTI-Horiba) using Xenon as a source.

3 Result and Discussion

3.1 Physical properties

Table 1. Physical properties of Nd_2O_3 concentration doped in barium oxide and oxy-fluoride borate glasses.

Optical Properties	One oxygen and one fluoride Glasses			Two fluoride Glasses
	BCaAlNaOBafNd$_{0.5}$ (F1)	**BCaAlNafBaONd$_{1.0}$ (R1)**	**BCaAlNafBafNd$_{0.5}$ (A3)**	**BCaAlNafBafNd$_{1.0}$ (F2)**
Density (g/cm^3)	2.8914	2.9019	2.7946	2.7484
Molar Volume	26.511	25.732	26.714	28.376
Refractive Index (n)	1.56	1.57	1.57	1.56
Dielectric constant(⊠)	2.4336	2.4336	2.4649	2.4649
Optical Thickness	0.400	0.412	0.423	0.377
Polaron radius R_p (Å)	3.915	3.104	3.959	3.161
Inter-ionic radii R_i (Å)	9.534	7.558	9.643	7.696

Continued on next page

Table 1 continued

Field strength ($\times 10^{20}$)	10.00	15.91	9.779	15.34

3.1.1 Analysis of physical properties (mass density, molar volume Vm and dielectric constant)

The mass density of glass samples has been listed in Table 1 along with the physical properties of

Neodymium doped Calcium Aluminum Barium Sodium Barium Fluoride Sodium Fluoride–Borate glasses. From the results, it's found that mass density and V_m rises from 2.25414(gm/kg^3) to 2.90193(gm/kg^3) and 25.7306(Cm^3/mol) to 40.7787(gm/kg^3) in accordance with the increase in mol concentration of Nd_2O_3 compositions. In The glass sample Nd_2O_3 concentration rises at the expense of B_2O_3 concentration. The increase molar weight of Nd_2O_3(336.48g/mol) which is greater than the molecular weight of the constituents in the glass samples accounts for the rise in glass density as (molecular weight of CaO, Al_2O_3, B_2O_3, BaO, Na_2O, BaF_2 and NaF are 56.08, 101.96, 69.6203, 153.33, 61.9789, 175.34, 41.998 g/mol respectively). Therefore, the glass network turns denser when Nd^{3+} ions are exchange internally along by B_2O_3. Whereas F1 glass show lower density and higher volume compared with other glasses suggesting a greater number of nonbridging oxygen's in the glass. The creation of non-bridging oxygen (NBO) and the expansion of CaAlBaNaBaFNaF borate glass network may be the causes of the rise in molar volume in the glass sample. The dielectric constant is somewhat increased by increasing the Nd_2O_3 content in the glass samples[8,9].

3.1.2 X-Ray Diffraction Studies

Figure 1 depicts the X-ray diffraction profiles of all the prepared glass samples doped with Nd^{3+} ions in present work. For all of the samples, the diffracted intensity was measured for the angular distribution of scattered x-ray energy between 10^0 and 100^0. Broad humps in the recorded XRD pattern plainly indicate that all of the manufactured Nd^{3+} doped glass samples are amorphous in nature[10].

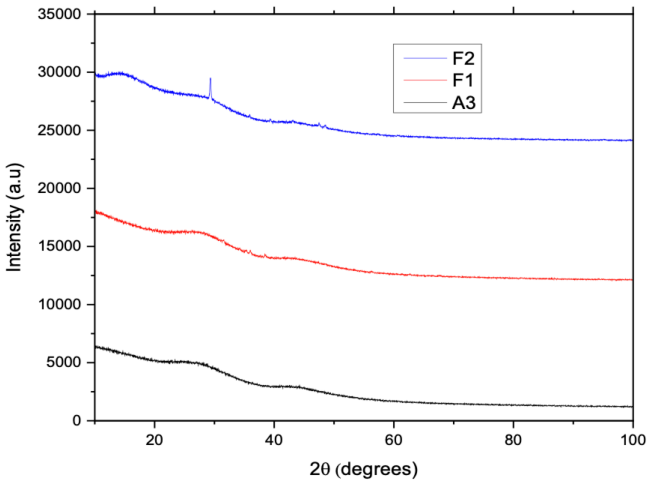

Fig 1. X-Ray diffraction pattern of prepared glasses

3.1.3 Optical Absorption studies

The absorbance studies of 23CaO; $10Al_2O_3$; (51- X) B_2O_3; $6BaF_2$; $10Na_2O$; XNd_2O_3 where, X=0.5, and 1.0, 23CaO; $10Al_2O_3$;

(51‑X) B_2O_3; 6BaF; 10NaF; XNd_2O_3 where X=0.5, and 23CaO; $10Al_2O_3$; (51-X) B_2O_3; 6BaO; 10NaF; XNd_2O_3 1.0, glass doped with various concentrations of Nd_2O_3. The Uv- visible NIR absorption spectrum of prepared glasses. The wavelength range of 400-900 nm, recorded at room temperature, is displayed in Figure 2. This absorption spectrum has 10 absorption bands and provides details on the non-crystalline material's band location, energy gap, and induced transitions. Centre around 430, 475, 511, 524, 583, 626, 681, 746 ,803 and 875 nm which corresponding to electronic transitions state of ($^2P_{1/2}$+$^2D5_{/2}$) , ($^2D_{3/2}$+$^{2G}9_{/2}$+$^2K_{15/2}$), $^4G_{9/2}$,$^4G_{7/2,}$ $^4G_{5/2}$+$^2G_{7/2}$), $^2H_{11/2,}$ $^4F_{9/2}$ ($^4S_3/_2$+$^4F_{7/2}$)

($^4_{F5/2+}$ $^2H_{9/2}$) and

$^4F_{3/2}$ respectively of Nd^{3+} ions in the glass

matrix. Electronic transition at $^4G_{5/2}$ + $^2G_{7/2}$ has highest intensityin the prepared glass samples at

626nm NIR region [11].

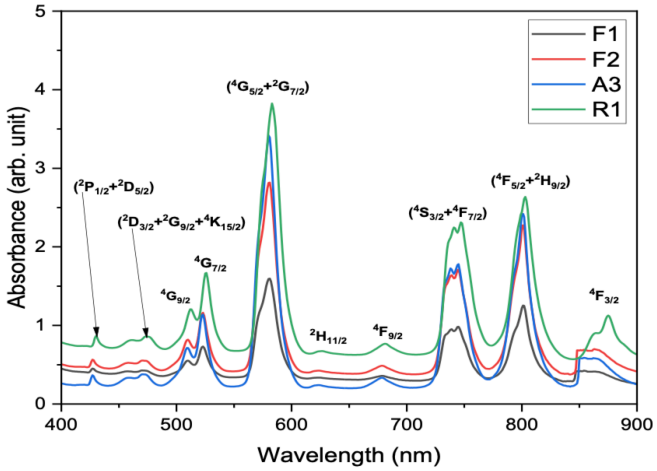

Fig 2. UV–Vis–NIR absorbance of BCaAlNaBaNd glasses

3.4 Luminescence studies

3.4.1 Photo-Emission spectra

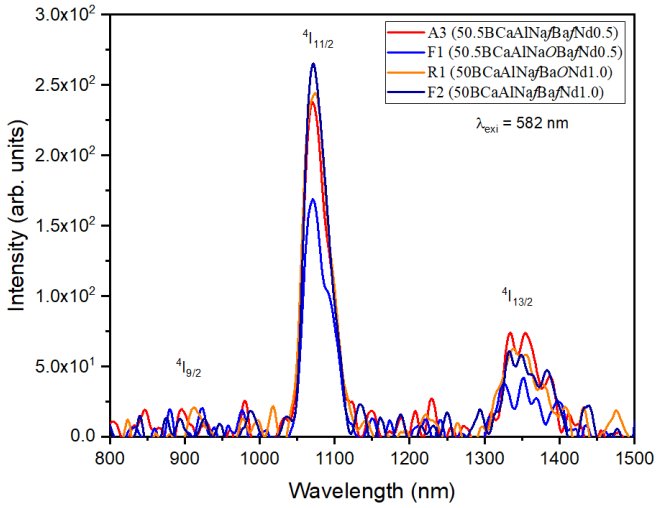

Fig 3. Photoluminescence Spectra of Emission ofBCaAlNaBaNd glasses

Figure 3 demonstrates the NIR emission spectra of BCaAlNaBaNd glasses stimulated with a 582nm laser diode and doped with various Nd^{3+} ion concentrations within the spectral range of 800nm to 1500nm. The spectra reveal three intense emission bands centered at 891, 1070 and 1335nm corresponding to the $^4F_{3/2}\rightarrow{}^4I_{9/2}$, $^4F_{3/2}\rightarrow{}^4I_{11/2}$, $^4F_{3/2}\rightarrow{}^4I_{13/2}$, emission transitions respectively. There may be a transition with a higher intensity than the other two in the entire emission band at 1069nm that corresponds to the $^4F_{3/2}\rightarrow{}^4I_{11/2}$ transition. It has been noted that as the concentration of neodymium ions increases, the emission intensity of the $^4F_{3/2}\rightarrow{}^4I_{11/2}$ transition increases up to 0.5 mol% Nd_2O_3 and thereafter decreases. The concentration quenching effect may be to blame for this [12,13]. The emission intensity of oxyfluoride glasses is higher than that of oxide glasses. The lower phonon energy of oxyfluoride glasses is likely to be responsible for the observed discrepancy between emission intensity. Since oxyfluoride glasses have better radiative emission characteristics than oxide glasses because their phonon energy is higher [14].

3.4.2 Judd-Ofelt Analysis

The J-O parameters clarify the glass network's structural characteristics, such as the type of bonding and rigidity. The table 2 displays the glass's BCaAlNaBaNd J-O measurements. As well as values for various other Nd^{3+} ion-doped CaAlBBaNaBaFNaF glasses that have been published in the literature. The J-O parameters are obtained for BCaAlNaBaNd glass are following the trends $\Omega_2>\Omega_6>\Omega_4$ and $\Omega_4>\Omega_6>\Omega_2$. Higher values of Ω_2 indicate non-symmetry in the crystal fields surrounding the location of Nd^{3+} ions as well as greater O-Nd covalency. table 3 reveals that the CaAlBBaNaBaFNaF (present) glass has greater Ω_2 values than some other host glasses. That shows more asymmetry of crystal field around Nd^{3+} ions in present glasses when compared with other glasses[7,15,16]. Through absorption spectrum, experimental oscillator strengths (f_{exp}) of the f-f transitions of were found and are used in the work of J-O theory, in the current glasses the $\Omega_2$parameter has the greater value compare to Ω_2 and $\Omega_6$the emission intensity through the $^4F_{3/2}$ level of Nd^{3+}ions can be unique characterized, Ω_4 and $\Omega_6$intensity parameters are spectroscopic quality factors. The current oxyfluoride glasses have higher values of Ω_2 than most of the glasses in table 3 and exhibit higher covalency of Nd-O bonds and greater site asymmetry of structure around Nd^{3+} ions. In a similar manner, Ω_4, Ω_6 are related to the bulk properties of glasses[14].

Table 2. Assignmentof absorption peaks of Nd^{3+} ions and their line strengths ($\times10^{-6}$) and JO parameters (Ω_λ where λ=2,4,6) glasses

Transition $^4I_{9/2}$	Level		A3		R1		F1		F2	
	(λ)	(cm^{-1})	f_{exp}	f_{cal}	f_{exp}	f_{cal}	f_{exp}	f_{cal}	f_{exp}	f_{cal}
$^4F_{3/2}$	854	11709	4.69	4.57	5.50	4.31	6.44	5.02	3.78	3.58
$^4F_{5/2}$, $^2H_{9/2}$	801	12484	10.3	9.80	7.20	2.28	8.89	9.33	6.14	6.52
$^4F_{7/2}$, $^4S_{3/2}$	745	13422	10.6	10.9	7.95	7.60	9.33	9.13	6.45	6.24
$^4F_{9/2}$	679	14727	0.31	0.87	0.41	0.64	052	0.77	0.29	0.53
$^2H_{11/2}$	624	16025	0.23	0.24	0.32	0.18	0.48	0.21	0.24	0.15
$^4G_{5/2,}$ $^2G_{7/2}$	581	17211	23.7	23.8	16.1	16.2	19.6	19.6	13.2	13.2
$^4G_{7/2,}$ $^4G_{9/2}$	523	19120	7.18	5.80	6.41	4.99	6.43	5.86	5.02	4.13
$^2G_{9/2,}$ $^2D_{3/2,}$ $^2K_{15/2}$	510	19607	0.53	0.73	0.52	0.45	0.79	0.55	0.40	0.37
	470	21276	1.57	1.75	1.73	1.56	2.54	1.83	1.51	1.29
$^2P_{1/2}$	429	23256	0.13	1.20	0.13	1.20	0.61	1.39	0.12	0.99
$^4D_{3/2,\ 5/2,}$ $^2I_{11/2,}$ $^2L_{15/2}$	353	28329	9.58	11.6	9.04	11.1	10.3	12.9	9.05	9.27
δ_{rms} ($\pm$)	11 transitions		0.866		0.945		0.996		0.420	
Ω_2 ($\times10^{-20}$) cm^2			9.236		9.231		10.77		9.605	
Ω_4 ($\times10^{-20}$) cm^2			2.944		0.190		5.661		7.733	
Ω_6 ($\times10^{-20}$) cm^2			7.475		4.995		6.072		4.128	
JO Trend			$\Omega_2>\Omega_6>\Omega_4$		$\Omega_2>\Omega_6>\Omega_4$		$\Omega_4>\Omega_6>\Omega_2$		$\Omega_2>\Omega_4>\Omega_6$	

Table 3. Absorption peaks of Nd^{3+} ions and their line strengths ($\times10^{-6}$) and JO parameters (Ω_λ where λ=2,4,6) glasses compared with other Nd^{3+} doped oxyfluoride glasses

Sl.No.	Glass	$\Omega_2(\times10^{20})$	$\Omega_4(\times10^{20})$	$\Omega_6(\times10^{20})$	J-O Trend	References
1	50.5BCaAlNafBafNd$_{0.5}$ (A3)	9.236	2.944	7.475	$\Omega_2>\Omega_6>\Omega_4$	Present Glass
2	50BCaAlNafBaONd$_{1.0}$ (R1)	9.231	0.190	4.995	$\Omega_2>\Omega_6>\Omega_4$	Present Glass
3	50.5BCaAlNaOBafNd$_{0.5}$ (F1)	10.77	5.661	6.072	$\Omega_2>\Omega_6>\Omega_4$	Present Glass
4	50BCaAlNafBafNd$_{1.0}$ (F2)	9.605	7.733	4.128	$\Omega_2>\Omega_4>\Omega_6$	Present Glass
5	Oxyfluoride Glass	9.83	5.69	12.64	$\Omega_6>\Omega_2>\Omega_4$	[12]
6	BaPbAlFBNd1.0	5.77	3.68	4.01	$\Omega_2>\Omega_6>\Omega_4$	[13]
7	TBZBNd0.5	2.89	1.35	1.59	$\Omega_2>\Omega_6>\Omega_4$	[14]
8	Nd05Eu000	3.09	2.83	1.31	$\Omega_2>\Omega_4>\Omega_6$	[15]
9	OFBNd0.5	8.18	5.35	3.57	$\Omega_2>\Omega_4>\Omega_6$	[16]
10	1.0mol%	8.55	11.54	10.25	$\Omega_4>\Omega_6>\Omega_2$	[17]

3.4.3 Radiative Properties

Calculations based on the absorption spectra were used to calculate the produced glass samples' radiative characteristics, such as their radiative transition probabilities (A_r), stimulated emission cross-sections (σ_e), branching ratios (β_{exp}, β_{cal}), radiative lifetime (τ_{rad}), and quantum efficiency (η) are tabulated in table.4. The computed radiative parameters all accord with the values found in the literature. The radiative emission spectra of all glasses are representing three emission bands correspondence to $^4F_{3/2} \rightarrow {}^4I_{9/2,}{}^4I_{11/2}$ and $^4I_{13/2}$ transitions are appearing around 900, 1066 and 1334 nm, respectively. Among these three bands $^4F_{3/2} \rightarrow {}^4I_{9/2}$ (900nm) is noticed that the most intense and $^4F_{3/2} \rightarrow {}^4I_{11/2}$(1334) nm is noticed that weak intensity compared to other glasses using the J-O theory and are tabulated in the table 4. The findings of the $^4F_{3/2} \rightarrow {}^4I_{11/2}$ transitions show that the A_R is2160 s^{-1} and 2398 s^{-1} for 0.5 and 0.5 mol% of Nd_2O_3 content in oxide (F1) and oxyfluoride (A3) glass respectively. The βCal and βExp are 0.44 and 0.43 respectively. The stimulated emission cross section σ_{emi}=29.9x10^{-21}cm^2 and σ_{emi}=32.5x10^{-21}cm^2 for oxide (F1) and oxy-fluoride (A3) glasses respectively. Similarly, for the $^4F_{3/2} \rightarrow {}^4I_{11/2}$ transitions showthat A_R is 1842 s^{-1} and1500 s^{-1} 1.0 and 1.0 mol% of Nd_2O_3 content in oxide (R1) oxyfluoride glasses (F2) respectively. The βCal are 0.43 and 0.43 respectively. The stimulated emission cross-section shows σ_{emi}=25.3x10^{-21}cm^2 and σ_{emi}=18.5x10^{-21}cm^2 for in oxide (R1) and oxy-fluoride glasses (F2) respectively. It is found that the oxy-fluoride glasses show higher stimulated emission cross section than compared to oxide glasses. When alkali ion oxygen is replaced by fluorine ion, they show more stimulated emission than compared to their oxygen counterpart. The quenching of emission intensity was not observed in the present case, the quenching can be observed due to energy transfer process through cross relaxation process [17,18]. Present samples retain their higher values of radiative properties for $^4F_{3/2} \rightarrow {}^4I_{11/2}$ transitions. One important factor that significantly influences lasing materials is the rate of energy extraction from a material, and the stimulated emission cross-section is a key measure for figuring out the rate of energy extraction. High optical gain materials require greater emission cross sections. Similar to this, the branching ratio is a crucial factor in determining if a certain transition has the potential for stimulated emission; it must be greater than 50% to be regarded suitable for laser applications. In our work the calculated values are more than 50% for $^4F_{3/2} \rightarrow {}^4I_{11/2}$ transition, hence the laser action is possible from $^4F_{3/2} \rightarrow {}^4I_{11/2}$ transition. table 5 show that oxyfluoride glasses exhibit greater values than oxide glasses at 1.6μm emission when compared among the samples and other reported literatures. As a result, the oxyfluoride glasses made in this work exhibit enhanced radiative characteristics and are therefore likely to be employed as a laser gain medium [7].

Table 4. Includes the following information: the emission band position (λp,nm), the stimulated emission cross-section ($\sigma_{emi} \times 10^{21}$ cm^2), the radiative transition probability (A_r, s^{-1}), the calculated and experimental branching ratio (β_{cal} and β_{exp}), radiative and experimental lifetime (τ in μs), and Quantum efficiency (η=τ_{exp}/ τ_{rad} (%)).

Transition	λp	σ_{emi}	A_r	β_{cal}	β_{exp}	τ_{rad}	τ_{exp}	η
50.5BCaAlNaOBafNd $_{0.5}$	**F1**							
$^4F_{3/2} \rightarrow {}^4I_{9/2}$	900	3.92	2585	0.50	0.011			
$^4F_{3/2} \rightarrow {}^4I_{11/2}$	1066	29.9	2160	0.44	0.730	195	91.7	47.0
$^4F_{3/2} \rightarrow {}^4I_{13/2}$	1334	1.90	345.8	0.06	0.258			
50BCaAlNafBaONd $_{1.0}$	**R1**							
$^4F_{3/2} \rightarrow {}^4I_{9/2}$	900	6.34	2247	0.50	0.022			
$^4F_{3/2} \rightarrow {}^4I_{11/2}$	1066	25.3	1842	0.43	0.719	227	63.7	28.0
$^4F_{3/2} \rightarrow {}^4I_{13/2}$	1334	11.7	290.3	0.06	0.258			
50.5BCaAlNafBafNd $_{0.5}$	**A3**							
$^4F_{3/2} \rightarrow {}^4I_{9/2}$	900	3.28	2381	0.45	0.031			
$^4F_{3/2} \rightarrow {}^4I_{11/2}$	1066	32.5	2398	0.45	0.674	190	62.9	33.1
$^4F_{3/2} \rightarrow {}^4I_{13/2}$	1334	17.8	434.5	0.08	0.294			
50BCaAlNafBafNd $_{1.0}$	**F2**							
$^4F_{3/2} \rightarrow {}^4I_{9/2}$	900	2.78	1842	0.49	0.021			
$^4F_{3/2} \rightarrow {}^4I_{11/2}$	1066	18.5	1500	0.43	0.720	278	61.3	22.0
$^4F_{3/2} \rightarrow {}^4I_{13/2}$	1334	9.41	235.1	0.06	0.258			

Table 5. Radiative properties of current glasses and compared with other Nd^{3+} doped glasses.

Glass	$\sigma(cm^2)$	A_r	β Cal	β Exp	
		λ=900 nm			
50.5BCaAlNaOBafNd$_{0.5}$ (F1)	3.92	2585	0.50	0.011	Present work
50BCaAlNafBaONd$_{1.0}$ (R1)	6.34	2247	0.50	0.022	Present work
50.5BCaAlNafBafNd$_{0.5}$ (A3)	3.28	2381	0.45	0.031	Present work
50BCaAlNafBafNd$_{1.0}$ (F2)	2.78	1842	0.49	0.021	Present work
SFB	0.91	1500	0.31	0.39	(3)
Oxyfluoride Glass	0.74	0933	0.2938	0.42	(12)
TBZBNd0.5	7.50	419.89	0.40	0.01	(14)
1.0mol%	6.06	2917	0.44	0.40	(17)
B70BINd$_{1.0}$	0.81	2511	0.42	0.35	(18)
PABLNd1.0	0.16	715.1	0.30	0.17	(19)
B35LC$_{of}$Nd$_{0.3}$	1.293	1412	0.471	0.425	(20)
BBaAZNd1.0	0.79	1419	0.39	0.37	(21)
		λ=1066nm			
50.5BCaAlNaOBafNd$_{0.5}$ (F1)	29.9	2160	0.44	0.730	Present work
50BCaAlNafBaONd$_{1.0}$ (R1)	25.3	1842	0.43	0.719	Present work
50.5BCaAlNafBafNd$_{0.5}$ (A3)	32.5	2398	0.45	0.674	Present work
50BCaAlNafBafNd$_{1.0}$ (F2)	18.5	1500	0.43	0.720	Present work
SFB	1.07	2666	0.55	0.50	(3)
Oxyfluoride Glass	5.65	2339	0.5686	0.51	(12)
TBZBNd0.5	9.07	516.3	0.5	0.72	(14)
1.0mol%	15.10	3091	0.47	0.54	(17)
B70BINd$_{1.0}$	3.15	2921	0.48	0.6	(18)
PABLNd1.0	8.53	1321.5	0.57	0.57	(19)
B35LC$_{of}$Nd$_{0.3}$	3.561	1585	0.528	0.478	(20)
BBaAZNd1.0	3.03	1842	0.51	0.54	(21)
		λ=1334nm			
50.5BCaAlNaOBafNd$_{0.5}$ (F1)	1.90	345.8	0.06	0.258	Present work
50BCaAlNafBaONd$_{1.0}$ (R1)	11.7	290.3	0.06	0.258	Present work
50.5BCaAlNafBafNd$_{0.5}$ (A3)	17.8	434.5	0.08	0.294	Present work
50BCaAlNafBafNd$_{1.0}$ (F2)	9.41	235.1	0.06	0.258	Present work
SFB	1.34	601	0.13	0.10	(3)
Oxyfluoride Glass	2.21	561	0.1311	0.07	(12)
TBZBNd0.5	3.46	102.91	0.10	0.27	(14)
1.0mol%	6.55	576	0.09	0.06	(17)
B70BINd$_{1.0}$	1.69	569	0.10	0.05	(18)
PABLNd1.0	3.29	301.1	0.13	0.26	(19)
B35LC$_{of}$Nd$_{0.3}$	1.003	304	0.101	0.091	(20)
BBaAZNd1.0	0.81	377	0.10	0.09	(21)

Table 6. Experimental lifetime (τ in μs), and Quantum efficiency (η=τ_{exp}/ τ_{rad} (%)) of current glasses and compared with other Nd^{3+}doped glasses

Glass	τ_{rad}	τ_{exp}	η	
50.5BCaAlNaOBafNd$_{0.5}$ (F1)	195	91.7	47.0	Present work
50BCaAlNafBaONd$_{1.0}$ (R1)	227	63.7	28.0	Present work
50.5BCaAlNafBafNd$_{0.5}$ (A3)	190	62.9	33.1	Present work
50BCaAlNafBafNd$_{1.0}$ (F2)	278	61.3	22.0	Present work
GeO2:TiO2 5:1	359	151	42	(2)
Oxyfluoride Glass	254	227	89.30	(12)
BBaAZNd1.0	275	52	19	(21)
PANCaFN1(0.5Nd^{3+})	295	141.62	48.01	(22)

3.2.4 Life time analysis

Experimental life times (τ_{exp}) is found to be 47, 33, 28 and 22μs for CaAlBNaBaFNd0.5CaAlBNaBaFNd1.0, CaAlBNaFBaFNd0.5 CaAlBNaFBaNd1.0, respectively. As a result of cross relaxation from $^4F_{3/2}$+$^4I_{9/2}$ to $^4I_{15/2}$+$^4I_{15/2}$, which is what reduces the life periods of $^4F_{3/2}$ level Nd^{3+}ions in the present glasses, energy is transferred from excited Nd^{3+} ions to ground state Nd^{3+} ions. As a result, the experimental life times (τ_{exp}) are decreased with increasing Nd_2O_3 concentration due to host defects in the glass structure Because of the high phonon energy of borate glass, it is found that all present glasses have radiative life times (τ_{rad}) that are longer than experimental life times (τ_{exp}). The ratio of experimental life times to radiative life times (τ_{exp}/τ_{rad}) is used to determine the quantum efficiency of the current glasses. As stated in table 6, BCaAlNaBaNd glasses have a quantum efficiency between 22% and 47%. The low efficiency of BCaAlNaBaNd glasses suggests that the borate glasses have more non-radiative transitional processes (21).

4 Conclusions

The glasses were synthesized with different variation of oxygen and fluorine content in the stoichiometry ratio. The oxide content glasses show more density that compared to fluorine content glasses. Judd-Ofelt analysis were employed to evaluate the JO parameters and follows the trends Ω2>Ω6>Ω4 and Ω4>Ω6>Ω2. It was found that higher intensity peak 1.06μm for higher fluorine content than compared to oxygen content. It was also, noted that the oxy-fluoride glasses show higher stimulated emission cross section than compared to oxide glasses. The present glasses show quantum efficiency around 22 to 47%. The data clearly suggests that addition of higher fluorine content in the glasses are suitable for NIR solid state device applications.

References

1) Lenkennavar SK, Eraiah B, Kokila MK. Rare earths doped oxy-fluoride glasses as candidates for generating tunable visible light. *Materials Today: Proceedings*. 2020;33:2550–2554. Available from: https://doi.org/10.1016/j.matpr.2019.12.066.
2) Pisarski WA, Kowalska K, Kuwik M, Pisarska J, Dorosz J, Zmojda J, et al. Nd3+ doped titanate-germanate glasses for near-IR laser applications. *Optical Materials Express*. 2022;12(7):2912–2912. Available from: https://doi.org/10.1364/OME.463478.
3) Lenkennavar SK. The synthesis and properties of oxyfluoride borate glasses incorporated with neodymium ion. *Journal of Scientific Research*. 2021;65(08):69–73. Available from: https://doi.org/10.1063/5.0002078.
4) Chialanza MR, Azcune G, Pereira HB, Gasparotto G, De Santana RC, Maia LJ, et al. Continuous trap distribution and variation of optical properties with concentration in oxi-fluoroborate glass doped with Nd3+. *Journal of Non-Crystalline Solids*. 2021;559:120683. Available from: https://doi.org/10.1016/j.jnoncrysol.2021.120683.
5) James JT, Jose JK, Manjunatha M, Suresh K, Madhu A. Structural, luminescence and NMR studies on Nd3+-doped sodium–calcium-borate glasses for lasing applications. *Ceramics International*. 2020;46(17):27099–27109. Available from: https://doi.org/10.1016/j.ceramint.2020.07.187.
6) Djamal M, Yuliantini L, Hidayat R, Rauf N, Horprathum M, Rajaramakrishna R, et al. Spectroscopic study of Nd3+ ion-doped Zn-Al-Ba borate glasses for NIR emitting device applications. *Optical Materials*. 2020;107:110018. Available from: https://doi.org/10.1016/j.optmat.2020.110018.
7) Rani PR, Venkateswarlu M, Swapna K, Mahamuda S, Talewar RA, Devi CBA, et al. NIR photoluminescence studies of Nd3+doped B2O3–BaF2–PbF2–Al2O3 glasses for 1.063 μm laser applications. *Journal of Luminescence*. 2021;229:117701. Available from: https://doi.org/10.1016/j.jlumin.2020.117701.
8) Kaewjaeng S, Kothan S, Chaiphaksa W, Chanthima N, Rajaramakrishna R, Kim HJ, et al. High transparency La2O3-CaO-B2O3-SiO2 glass for diagnosis x-rays shielding material application. *Radiation Physics and Chemistry*. 2019;160:41–47. Available from: https://doi.org/10.1016/j.radphyschem.2019.03.018.
9) Shaaban MH, Rammah YS, Ahmed EM, Ali AA. Fabrication, physical, thermal and optical properties of oxyfluoride glasses doped with rare earth oxides. *Journal of Materials Science: Materials in Electronics*. 2021;32(14):18951–18967. Available from: https://link.springer.com/content/pdf/10.1007/s10854-021-06410-7.
10) Kashif I, Ratep A. ICMMS-2: Influences the Addition of Neodymium Oxide on Structural and Optical Properties of Oxyfluoride Lead Borate Glass. *Egyptian Journal of Chemistry*. 2021;64(3):1141–1147. Available from: https://doi.org/10.21608/ejchem.2021.55860.3183.

11) Rao KV, Babu S, Balanarayana C, Ratnakaram YC. Comparative impact of Nd3+ ion doping concentration on near-infrared laser emission in lead borate glassy materials. *Optik*. 2020;202:163562. Available from: https://doi.org/10.1016/j.ijleo.2019.163562.
12) Sreedhar VB, Doddoji R, Kumar KK, Reddy VRM. A study of NIR emission and associated spectroscopic properties of Nd3+:P2O5+K2O+Al2O3+ZnF2 glasses for 1.06 μm laser applications. *Journal of Non-Crystalline Solids*. 2021;553:120521. Available from: https://doi.org/10.1016/j.jnoncrysol.2020.120521.
13) Kumar M, Ratnakaram YC. Role of TeO2 coordination with the BaF2 and Bi2O3 on structural and emission properties in Nd3+ doped fluoro phosphate glasses for NIR 1.058 μm laser emission. *Optical Materials*. 2021;112:110738. Available from: https://doi.org/10.1016/j.optmat.2020.110738.
14) Shoaib M, Rooh G, Chanthima N, Sareein T, Kim HJ, Kothan S, et al. Luminescence behavior of Nd3+ions doped ZnO-BaO-(Gd2O3/GdF3)- P2O5 glasses for laser material applications. *Journal of Luminescence*. 2021;236:118139. Available from: https://doi.org/10.1016/j.jlumin.2021.118139.
15) Yuliantini L, Djamal M, Hidayat R, Boonin K, Kaewkhao J, Yasaka P. Luminescence and Judd-Ofelt analysis of Nd3+ ion doped oxyfluoride boro-tellurite glass for near-infrared laser application. *Materials Today: Proceedings*. 2021;43:2655–2662. Available from: https://doi.org/10.1016/j.matpr.2020.04.631.
16) Umamaheswar G, Gelija D, Rajesh M, Sushma NJ, Gowthami T, Nagajyothi PC, et al. Effect of Eu3+ ions on optical and fluorescence studies of Nd3+ ions doped zinc-lithium fluoroborate glasses. *Journal of Luminescence*. 2019;207:201–208. Available from: https://doi.org/10.1016/j.jlumin.2018.11.015.
17) Kumar KU, Babu P, Basavapoornima C, Praveena R, Rani DS, Jayasankar CK. Spectroscopic properties of Nd3+-doped boro-bismuth glasses for laser applications. *Physica B: Condensed Matter*. 2022;646:414327. Available from: https://doi.org/10.1016/j.physb.2022.414327.
18) Thongyoy P, Kedkaew C, Meejitpaisan P, Minh PH, Keawmon T, Rajaramakrishna R, et al. 1.06 μm emission of Nd3+-doped aluminium barium lithium phosphate glasses for near IR laser medium material. *Optik*. 2022;269:169852. Available from: https://doi.org/10.1016/j.ijleo.2022.169852.
19) Venugopal AR, Rajaramakrishna R, Rajashekara KM, Pattar V, Wongdamnern N, Kothan S, et al. Nd3+ doped B2O3+ Li2O+ CaO+ CaF2 glass systems: Structural and optical properties. *Optical Materials*. 2022;133:112979. Available from: https://doi.org/10.1016/j.optmat.2022.112979.
20) Shoaib M, Rooh G, Chanthima N, Kim HJ, Kaewkhao J. Luminescence properties of Nd3+ ions doped P2O5-Li2O3-GdF3 glasses for laser applications. *Optik*. 2019;199:163218. Available from: https://doi.org/10.1016/j.ijleo.2019.163218.
21) Rajagukguk J, Situmorang R, Fitrilawati, Djamal M, Rajaramakrishna R, Kaewkhao J, et al. Structural, spectroscopic and optical gain of Nd3+ doped fluorophosphate glasses for solid state laser application. *Journal of Luminescence*. 2019;216:116738. Available from: https://doi.org/10.1016/j.jlumin.2019.116738.
22) Venkateswarlu M, Swapna K, Mahamuda S, Rani PR, Kumar JVS, Prasad MVVKS, et al. Concentration dependent neodymium doped oxy fluoroborate glasses for 1.08 μm laser applications. *Solid State Sciences*. 2021;113:106543. Available from: https://doi.org/10.1016/j.solidstatesciences.2021.106543.